



## EFFECT OF FE ADDITION TOWARDS $\text{TiO}_2$ FORMATION FOR PHOTOCATALYTIC ACTIVITY

Khoo Ming Teck and Siti Aida Ibrahim

Faculty of Mechanical and Manufacturing Engineering, Universiti Tun Hussein Onn Malaysia

E-Mail: [saida@uthm.edu.my](mailto:saida@uthm.edu.my)

### ABSTRACT

Titanium dioxide ( $\text{TiO}_2$ ) is one of the basic ceramic material which has found involves in variety of application in industry and in our daily life. The size of nano  $\text{TiO}_2$  proves has great potential of improvement in physical, optical, biological and electrical properties. The main purpose of this work is to investigate the effect of Fe incorporated  $\text{TiO}_2$  with Fe amount varied from 0.5 to 1.5 mol %. In this work, Fe- $\text{TiO}_2$  nano powder was synthesized via sol gel method and subsequently followed by calcination process at 500 °C for 2 hours. The as-prepared samples were characterized by x-ray diffraction (XRD), energy dispersive x-ray spectroscopy (EDX), field emission scanning electron microscope (FESEM) and ultraviolet-visible spectrophotometer (UV-Vis). The results obtained from XRD showed the presence of anatase phase in all samples. FESEM images revealed that all samples were agglomerated with irregular shape while EDX analysis confirmed the presence of titanium, oxygen and iron in the samples. UV-Vis results exhibited that the wavelength threshold was shifted to 566 nm as the amount of Fe was increased to 1.5 mol% Fe. The band gap energy of Fe- $\text{TiO}_2$  was ranging from 2.6 eV to 2.9 eV indicating that Fe- $\text{TiO}_2$  has high potential for visible response photocatalyst.

**Keywords:**  $\text{TiO}_2$  synthesis, sol-gel method, photocatalytic activity.

### INTRODUCTION

The rapid growth of industries especially in developed countries has lead to the expansion of environmental problems. Industries such as textile, food, printing and others have cause environmental problems due to the disposal of toxic waste, dyes and other pollutant into water and air which can bring harm towards human being and ecosystem. (Afroz *et al.* 2003, Beatty and Shimshack, 2014, Herrmann *et al.* 2007). To improve the air and water quality, extensive research work by various researchers comes out with plenty technologies such as the usage of tree as bio-indicator for heavy metal (Sawidis *et al.* 2011), filtration (Hedberg *et al.* 2011) and oxidation process (Deiber *et al.* 1997, Magureanu *et al.* 2005, Arslan-Alaton, 2007). However, not all methods mentioned above can be used in various environments. Some method is very expensive, applicable only in selective environment or condition, high maintenance and difficult to handle. Therefore, scientist continuously looking and developing new ways to address this issue.

Based on literatures review, the developments of new catalytic and photocatalytic processes provide great help to address this problem. Lloyd (2006) reported that these material based-catalyst has great potential in controlling water contaminant or air pollutants. The advantages of using these type materials over conventional oxidation process are: (1) complete mineralization of the pollutants; (2) use near UV or solar light; (3) can be operated in room temperature, (4) safe, clean and efficient and (5) easily co-exist harmoniously with the environment (Herrmann, 1999, Anpo and Takeuchi, 2003, Catalkaya and Kargi, 2007, Zhai *et al.* 2010).

One of the promising material based-catalyst is titanium dioxide ( $\text{TiO}_2$ ).  $\text{TiO}_2$  is a semiconductor photocatalyst and has been proven suitable for various

environmental applications due to its stability, strong oxidizing powers, non-toxicity materials, ready availability and low cost (Chen and Mao, 2007, Nakata and Fujishima, 2012, Sin *et al.* 2011). As photocatalyst,  $\text{TiO}_2$  required the presence of light to decompose organic materials.  $\text{TiO}_2$  can be classified into three structure which are anatase, rutile and brookite. Among these three, anatase is proven to be most excellent photocatalyst as an excellent photocatalyst when compared to rutile and brookite. It is reported that high crystallinity of anatase offers fewer defects acting as recombination sites between photogenerated electrons and holes. In another study Luttrell *et al.* (2014) described that the lifetime of charge carriers is high in anatase when compared to rutile, indicating high photocatalytic activity. On the other hand, brookite is seldom studied due to its complicated synthesis procedure (Di Paola *et al.* 2013).

However,  $\text{TiO}_2$  is only active under UV light irradiation due to its large band gap energy (3.2 eV), which results in a low efficiency to make use of solar light. Significantly efforts have been made in the past decades to develop  $\text{TiO}_2$  based photo catalysts capable of using abundant visible light in solar radiation or artificial light. To improve the absorption wave length range of  $\text{TiO}_2$  higher toward visible region, many attempt on surface modification such as metal ion and non-metal doping or coupling it with other narrow band gap semiconductors (Akpan and Hameed, 2010, Pelaez *et al.* 2012). Several literatures were found to incorporate  $\text{TiO}_2$  with metal ion such as  $\text{Ag}^+$ ,  $\text{Cu}^{2+}$ ,  $\text{Fe}^{3+}$  and  $\text{Zr}^{4+}$  on  $\text{TiO}_2$  (Naraginti *et al.* 2015, Ibrahim and Sreekantan, 2014, Behnajady and Eskandarloo, 2013). Among transitional metal ions have been used as dopant in  $\text{TiO}_2$  system, Fe is extensively used as it is believed that  $\text{Fe}^{3+}$  can trap photo generated electrons and transfer them to pre-absorbed species to form active species, whereas surface  $\text{Fe}^{3+}$  sites



can trap holes. These different roles of Fe<sup>3+</sup> increase the efficiency of charge separation and transfer of Fe-TiO<sub>2</sub> and thus promote the selective photo catalytic oxidation of pollutant under visible light irradiation (Sun *et al.* 2012).

There are various method can be conducted to synthesis TiO<sub>2</sub>. Method such as hydrothermal, chemical vapor deposition and sol-gel techniques are widely in order to synthesize nanocrystalline TiO<sub>2</sub> (Du *et al.* 2011, Attar *et al.* 2011, Elghniji *et al.* 2012). Sol gel technique has been adopted as one of the versatile methods for the preparation of metal and nonmetal doped nano crystalline TiO<sub>2</sub>. Since this method is a solution process, it allows flexibility in parameter control with its relatively slow reaction process. This permits tailoring of certain structural characteristics such as compositional homogeneity, grain size, particle morphology and porosity (Hamadani *et al.* 2011).

In this work, TiO<sub>2</sub> and Fe-TiO<sub>2</sub> nano powder were synthesized by sol gel method by using titanium (iv) isopropoxide and iron (iii) nitrate as precursor. The synthesized TiO<sub>2</sub> and Fe-TiO<sub>2</sub> were characterized by x-ray diffraction (XRD), energy dispersive x-ray spectroscopy (EDX), field emission scanning electron microscope (FESEM) and ultraviolet-visible spectrophotometer (UV-VIS).

## METHODOLOGY

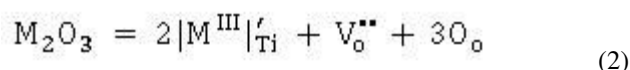
The pure TiO<sub>2</sub> and Fe-TiO<sub>2</sub> nano powder were prepared by a sol gel method using titanium(iv) isopropoxide (TTIP) and iron(iii) nitrate as the precursor of Ti and Fe, respectively precursor. The detailed procedure was as follow: 20 ml titanium (iv) isopropoxide was dissolved in 80 ml isopropanol and the obtained solution was added drop wise into hydrolysis medium containing 80 ml isopropanol, 6 ml distilled water and 8 ml acetic acid under vigorous stirring. The resultant transparent colloid suspension was stirred for 3 h and centrifuged at 9000 rpm for 10 min. The gel was dried in oven at 80 °C for 12 h. The dried powder was calcined at 500 °C for 2 h to obtain pure TiO<sub>2</sub> nano powder. For the Fe-TiO<sub>2</sub> nano powder, the ion Fe was incorporated into TiO<sub>2</sub> by adding certain amount of iron(iii) nitrate according the desired mol % Fe (0.5, 0.75, 1.0 and 1.5 mol %) in the hydrolysis medium during synthesis process.

The as-prepared samples were characterized by x-ray diffraction (XRD), energy dispersive x-ray spectroscopy (EDX), field emission scanning electron microscope (FESEM) and ultraviolet-visible spectrophotometer (UV-VIS). The XRD was performed on a D8 Advanced Bruker System with Cu K $\alpha$  radiation as the x-ray source. The crystallite sizes of samples were calculated using Debye-Scherrer equation with correction for instrumental line broadening. Morphologies of the samples were observed by using high resolution field emission environmental scanning electron microscope (FESEM, JSM-7600F). Optical properties of samples were measured on a Shimadzu UV-VIS spectrometer (UV-1800) in the wavelength of 300-800 nm.

## RESULTS AND DISCUSSION

The structure and crystalline size of nano TiO<sub>2</sub> and Fe-TiO<sub>2</sub> are determined using XRD technique. As observed in Figure-1, the diffraction peak of all samples were similar to anatase phase (JCPDS Card No: 21-1272). The peaks are located at the 2 $\theta$  values of 25.4 $^{\circ}$ , 37.9 $^{\circ}$ , 47.9 $^{\circ}$ , 53.9 $^{\circ}$ , 54.9 $^{\circ}$  and 62.7 $^{\circ}$  corresponding to plane (101), (004), (200), (105), (211) and (204) crystal phase, respectively. It was found that the incorporation of Fe did not affect the structure of TiO<sub>2</sub> (anatase) although Fe amount was increased. In addition, no peak that associated with Fe was observed even at high concentration of 1.5 mol % Fe. This may due to two reasons, one is the limitation of XRD to detect low concentration of Fe in the composition used and the other one is the similarity of ionic radius size between Ti<sup>4+</sup> (0.68 Å) and Fe<sup>3+</sup> (0.64 Å) (Safari *et al.* 2013, Jamalluddin and Abdullah, 2011).

Kment *et al.* (2010) reported that the substitution of metal ion in TiIV sites in lattice is possible when the ionic radius of both metal ion and host metal are identical in size. Serpone *et al.* (1994) reported that incorporating TiO<sub>2</sub> with metal ion with trivalent charge such as Cr and Fe that could substitutionally located in TiIV lattice sites with or without charge compensation by an oxygen vacancy, V<sub>O</sub><sup>••</sup>, at a nearest neighbor site about below 0.08 eV below ECB. However, in order for electroneutrality, the number of oxygen vacancies generated by metal doping need to be half the number of substitutional trivalent cations at TiIV sites, |M<sup>III</sup>|<sub>Ti</sub> as shown in equation 2.



where O<sub>O</sub> denotes an oxygen atom at its normal lattice site; A fraction of the |M<sup>III</sup>|<sub>Ti</sub> centers have a full coordination sphere of lattice oxygen (tetragonal symmetry) while the fraction of charge compensated centers, M<sub>cc</sub><sup>III</sup>, have an oxygen vacancy at a nearest neighbor site (lower symmetry). To note, the presence of oxygen vacancies are required for better performance of TiO<sub>2</sub> photocatalytic activity. Therefore, in this work, it is possible that Fe<sup>3+</sup> might sit in Ti<sup>IV</sup> sites in TiO<sub>2</sub> lattice due to similarity of ionic radius in size.

Based from the XRD pattern (Figure-1), it is observed that the prepared samples have broader peaks indicating the crystallite size is in nanoscale size. The crystallite size was calculated using Debye-Scherrer equation as described in equation 1 (Sayyar *et al.* 2015).

$$D = \frac{K\lambda}{\beta \cos \theta} \quad (1)$$

where D denotes as the average crystallite size (nm); K is the Scherrer constant, somewhat arbitrary value that falls in the range 0.8–1.0 (it assumed to be 0.9 in present work);  $\lambda$  is wavelength of X-ray radiation (0.154 nm);  $\theta$  is the diffraction angle and  $\beta$  is full width at half maximum (FWHM). The calculated value of the crystallite



size for  $\text{TiO}_2$  and Fe incorporated  $\text{TiO}_2$  nanoparticles were in the range of 14 to 16 nm and summarized in Table-1.

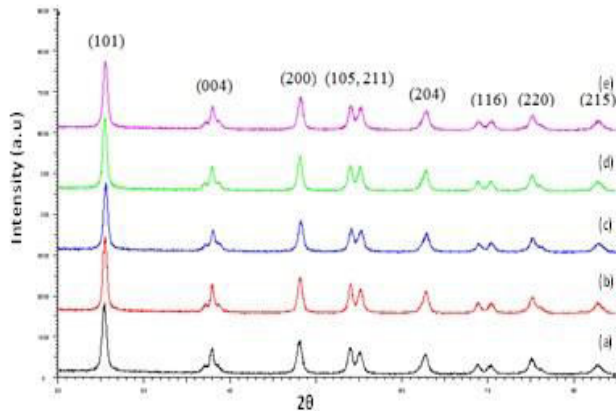


**Figure-1.** XRD diffractogram of  $\text{TiO}_2$  using (a) pure  $\text{TiO}_2$ , (b) 0.5 mol% Fe, (c) 0.75 mol% Fe, (d) 1 mol% Fe and (e) 1.5 mol% Fe.

**Table 1.** The characteristic of  $\text{TiO}_2$  and Fe incorporated  $\text{TiO}_2$  synthesized using sol-gel method and calcined at 500 °C for 2 h.

Samples	Fe amount (mol%)	Phase	Crystallite size (nm)	Absorption Wavelength (nm)
Pure $\text{TiO}_2$	0	Anatase	14.79	391
0.5% Fe- $\text{TiO}_2$	0.5	Anatase	15.11	475
0.75% Fe- $\text{TiO}_2$	0.75	Anatase	14.95	513
1.0 % Fe- $\text{TiO}_2$	1.0	Anatase	15.61	545
1.5% Fe- $\text{TiO}_2$	1.5	Anatase	14.20	566

The morphology of the sample was observed via FESEM. The FESEM images are shown in Figure-2. Based from Figure-2, it is clearly observed that  $\text{TiO}_2$  and Fe- $\text{TiO}_2$  samples were agglomerated and in irregular shape. The average particle size of  $\text{TiO}_2$  was estimated to be 28.4 nm while Fe- $\text{TiO}_2$  was about 16.9 nm. The agglomeration of particles may occur due to several reasons such as the presence of capillary absorption, solid bridge, Van der Waals and hydrogen bond (Su *et al.* 2011). In addition, Brinker and Scherer (1990) reported that small particles incline to agglomerate due to the high surface energy and this occurrence draws other particles to coalesce together and formed larger particles size.

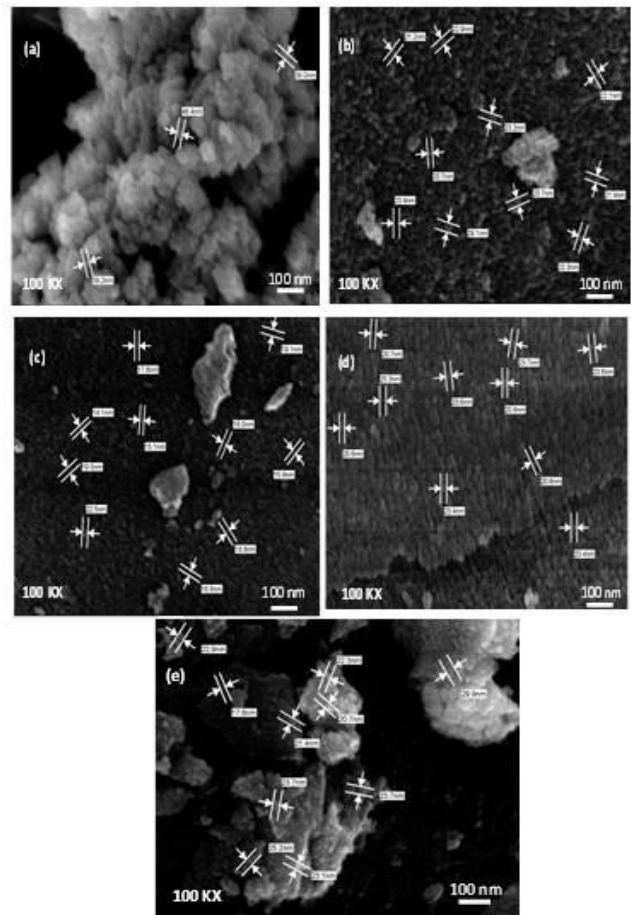


**Figure-2.** FESEM images of  $\text{TiO}_2$  and Fe- $\text{TiO}_2$  with (a) pure  $\text{TiO}_2$ , (b) 0.5 mol% Fe, (c) 0.75 mol% Fe (d) 1 (e) 1.5 mol % Fe.

EDX analysis was conducted in order to investigate the distribution for elements presence in the prepared samples. The atomic percentage of elements presence in the synthesized samples are lists in Table-2. It was confirmed the presence of Fe element in Fe- $\text{TiO}_2$  samples. This indicated that Fe was successfully incorporated into  $\text{TiO}_2$  particles as the Fe atomic percentage was increased as the amount of mol% Fe was increased during synthesis process.

**Table-2.** The atomic percentage of the elements in the  $\text{TiO}_2$  and Fe- $\text{TiO}_2$  nanoparticles.

samples	Atomic Percentage (%)			Total (%)
	Ti	O	Fe	
Pure $\text{TiO}_2$	41.98	58.02	0	100
0.5% Fe- $\text{TiO}_2$	30.61	69.10	0.29	100
0.75% Fe- $\text{TiO}_2$	35.45	64.08	0.46	100
1.0% Fe- $\text{TiO}_2$	40.56	58.83	0.60	100
1.5% Fe- $\text{TiO}_2$	40.03	59.17	0.80	100



In order to investigate the light absorption characteristic of Fe-TiO<sub>2</sub>, UV-Vis diffuse reflectance was conducted and the result obtained is illustrated in Figure-3. Based on previous study, the absorption edge of pure TiO<sub>2</sub> was 391 nm. Meanwhile, the incorporation of Fe into TiO<sub>2</sub> was successfully extended the absorption wavelength into visible region. It was found that Fe incorporation red-shifted to visible region in the range of 470 to 570 nm (Table-1). The values of the light absorption was obtained by extrapolating the steepest slope of the UV-Vis spectra. The intersection point between X-axis and the extrapolation line shows the excitation wavelength of Fe-TiO<sub>2</sub>. According to Reddy *et al.* (2003) and Naraginti *et al.* (2015), the band gap energy ( $E_g$ ) could be calculated using equation.

$$(\alpha h\nu)^2 = A(h\nu - E_g)^n \quad (3)$$

Where  $\alpha$  is the absorption coefficient, A is a constant, and  $n = 2$  for direct transition or  $n = 1/2$  for indirect transition.

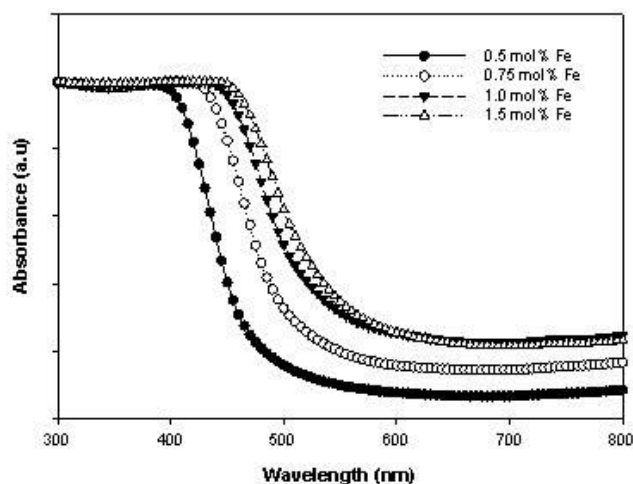


Figure-3. Optical property of Fe-TiO<sub>2</sub> calcined at 400° C.

The band gap energy ( $E_g$ ) was derived by the extrapolation of Kubelka-Munk plot of  $h\nu$  vs.  $(\alpha h\nu)^{1/2}$ . The  $E_g$  calculated using indirect transition gave an appropriate result compared to direct transition. The  $E_g$  values of 0.5 mol % Fe-TiO<sub>2</sub>, 0.75 mol % Fe-TiO<sub>2</sub>, 1.0 mol % Fe-TiO<sub>2</sub> and 1.5 mol % Fe-TiO<sub>2</sub> were estimated to be 2.90 eV, 2.82 eV, 2.75 eV and 2.69 eV, respectively. The results suggested that the incorporation of Fe extends the light absorption of pure TiO<sub>2</sub> to visible range. This result is similar to Castro *et.al* as the absorption threshold was shifted into the visible region. This is attributed to the excitation of 3d electrons of the Fe<sup>3+</sup> transferring from the energy level of the dopant to the conduction band of the TiO<sub>2</sub>. Further investigation by Yu *et al.* (2009) using density functional theory (DFT) calculation confirmed that the red shift of absorption edges and the narrowing of band gap energy for Fe doped TiO<sub>2</sub>. They found that the energy level of Fe 3d were lower than Ti 3d at the bottom

of CB with a decreased about 0.2 to 0.34 eV. Thus the electron transition from VB to CB had a decrease about 0.2 to 0.34 eV which induced a red shift of an optical absorption edge. Based on these result, it clearly seen that the amount of Fe added into TiO<sub>2</sub> was responsible for the decreased of bandgap energy. This indicated that the presence of Fe probably influences the photo catalytic activity of TiO<sub>2</sub> under visible light region.

## CONCLUSIONS

In conclusion, TiO<sub>2</sub> and 0.5 to 1.5 mol % Fe-TiO<sub>2</sub> were successfully synthesized via sol gel process and characterized by x-ray diffraction (XRD), field emission electron microscopy (FESEM), energy dispersive x-ray spectroscopy (EDX) and uv-visible spectroscopy (UV-VIS). The XRD result shown that obtained diffraction peak of sample TiO<sub>2</sub> and Fe-TiO<sub>2</sub> were anatase with crystallite size ranging from 14 to 16 nm. The micrograph images indicated that the samples are agglomerated due to small particle size. The UV-Vis analysis indicated that the increased amount Fe caused the wavelength of samples extended in the visible light region from 475 nm to 566 nm with band gap energy ranging from 2.6 eV to 2.9 eV, which is lower than pure TiO<sub>2</sub> (3.2 eV). This indicated that Fe incorporation with TiO<sub>2</sub> may increase the photocatalyst activity of TiO<sub>2</sub> under visible light irradiation.

## ACKNOWLEDGEMENTS

The authors would like to express their greatest acknowledgments to Universiti Tun Hussein Onn for funding support through Short Term Grant Scheme (STG) Vot 1334.

## REFERENCES

- [1] Afroz, R., Hassan, M. N. & Ibrahim, N. A. 2003. Review of air pollution and health impacts in Malaysia. *Environmental research*, 92, 71-77.
- [2] Akpan, U. G. & Hameed, B. H. 2010. The advancements in sol-gel method of doped-TiO<sub>2</sub> photocatalysts. *Applied Catalysis A: General*, 375, 1-11.
- [3] Anpo, M. & Takeuchi, M. 2003. The design and development of highly reactive titanium oxide photocatalysts operating under visible light irradiation. *Journal of catalysis*, 216, 505-516.
- [4] Arslan-Alaton, I. 2007. Degradation of a commercial textile biocide with advanced oxidation processes and ozone. *Journal of Environmental Management*, 82, 145-154.
- [5] Attar, A., Halali, M., Sobhani, M. & Ghandehari, R. T. 2011. Synthesis of titanium nano-particles via chemical vapor condensation processing. *Journal of Alloys and Compounds*, 509, 5825-5828.



- [6] Beatty, T. K. M. & Shimshack, J. P. 2014. Air pollution and children's respiratory health: A cohort analysis. *Journal of Environmental Economics and Management*, 67, 39-57.
- [7] Behnajady, M. A. & Eskandarloo, H. 2013. Silver and copper co-impregnated onto TiO<sub>2</sub>-P25 nanoparticles and its photocatalytic activity. *Chemical Engineering Journal*, 228, 1207-1213.
- [8] Brinker, C. J. & Scherer, G. W. 1990. *Sol-gel science: the physics and chemistry of sol-gel processing*, Academic Pr.
- [9] Catalkaya, E. C. & Kargi, F. 2007. Color, TOC and AOX removals from pulp mill effluent by advanced oxidation processes: A comparative study. *Journal of Hazardous Materials*, 139, 244-253.
- [10] Chen, X. & Mao, S. S. 2007. Titanium dioxide nanomaterials: synthesis, properties, modifications, and applications. *Chemical reviews*, 107, 2891-2959.
- [11] Deiber, G., Foussard, J. N. & Debellefontaine, H. 1997. Removal of nitrogenous compounds by catalytic wet air oxidation. Kinetic study. *Environmental Pollution*, 96, 311-319.
- [12] DI Paola, A., Bellardita, M. & Palmisano, L. 2013. Brookite, the Least Known TiO<sub>2</sub> Photocatalyst. *Catalysts*, 3, 36-73.
- [13] DU, J., Chen, W., Zhang, C., Liu, Y., Zhao, C. & DAI, Y. 2011. Hydrothermal synthesis of porous TiO<sub>2</sub> microspheres and their photocatalytic degradation of gaseous benzene. *Chemical Engineering Journal*, 170, 53-58.
- [14] Elghniji, K., Ksibi, M. & Elaloui, E. 2012. Sol-gel reverse micelle preparation and characterization of N-doped TiO<sub>2</sub>: Efficient photocatalytic degradation of methylene blue in water under visible light. *Journal of Industrial and Engineering Chemistry*, 18, 178-182.
- [15] Hamadani, M., Reisi-Vanani, A., Behpour, M. & Esmaeily, A. S. 2011. Synthesis and characterization of Fe,S-codoped TiO<sub>2</sub> nanoparticles: Application in degradation of organic water pollutants. *Desalination*, 281, 319-324.
- [16] Hedberg, Y., Herting, G. & Wallinder, I. O. 2011. Risks of using membrane filtration for trace metal analysis and assessing the dissolved metal fraction of aqueous media – A study on zinc, copper and nickel. *Environmental Pollution*, 159, 1144-1150.
- [17] Herrmann, J.-M. 1999. Heterogeneous photocatalysis: fundamentals and applications to the removal of various types of aqueous pollutants. *Catalysis Today*, 53, 115-129.
- [18] Herrmann, J. M., Duchamp, C., Karkmaz, M., Hoai, B. T., Lachheb, H., Puzenat, E. & Guillard, C. 2007. Environmental green chemistry as defined by photocatalysis. *Journal of Hazardous Materials*, 146, 624-629.
- [19] Ibrahim, S. A. & Sreekantan, S. Fe-TiO<sub>2</sub> Nanoparticles by Hydrothermal Treatment with Photocatalytic Activity Enhancement. *Advanced Materials Research*, 2014. Trans Tech Publ, 39-43.
- [20] Jamalluddin, N. A. & Abdullah, A. Z. 2011. Reactive dye degradation by combined Fe(III)/TiO<sub>2</sub> catalyst and ultrasonic irradiation: Effect of Fe(III) loading and calcination temperature. *Ultrasonics Sonochemistry*, 18, 669-678.
- [21] Kment, S., Kmentova, H., Kluson, P., Krysa, J., Hubicka, Z., Cirkva, V., Gregora, I., Solcova, O. & Jastrabik, L. 2010. Notes on the photo-induced characteristics of transition metal-doped and undoped titanium dioxide thin films. *Journal of Colloid and Interface Science*, 348, 198-205.
- [22] Lloyd, L. 2006. *Handbook of Industrial Catalysts*, Springer Science + Business Media.
- [23] Luttrell, T., Halpegamage, S., Tao, J., Kramer, A., Sutter, E. & Batzill, M. 2014. Why is anatase a better photocatalyst than rutile?-Model studies on epitaxial TiO<sub>2</sub> films. *Scientific reports*, 4.
- [24] Magureanu, M., Mandache, N. B., Eloy, P., Gaigneaux, E. M. & Parvulescu, V. I. 2005. Plasma-assisted catalysis for volatile organic compounds abatement. *Applied Catalysis B: Environmental*, 61, 12-20.
- [25] Nakata, K. & Fujishima, A. 2012. TiO<sub>2</sub> photocatalysis: Design and applications. *Journal of Photochemistry and Photobiology C: Photochemistry Reviews*, 13, 169-189.
- [26] Naraginti, S., Stephen, F. B., Radhakrishnan, A. & Sivakumar, A. 2015. Zirconium and silver co-doped TiO<sub>2</sub> nanoparticles as visible light catalyst for reduction of 4-nitrophenol, degradation of methyl orange and methylene blue. *Spectrochimica Acta Part A: Molecular and Biomolecular Spectroscopy*, 135, 814-819.
- [27] Pelaez, M., Nolan, N. T., Pillai, S. C., Seery, M. K., Falaras, P., Kontos, A. G., Dunlop, P. S. M., Hamilton, J. W. J., Byrne, J. A., O'shea, K., Entezari, M. H. & Dionysiou, D. D. 2012. A review on the visible light active titanium dioxide photocatalysts for



environmental applications. *Applied Catalysis B: Environmental*, 125, 331-349.

- [28] Reddy, K. M., Manorama, S. V. & Reddy, A. R. 2003. Bandgap studies on anatase titanium dioxide nanoparticles. *Materials Chemistry and Physics*, 78, 239-245.
- [29] Safari, M., Nikazar, M. & Dadvar, M. 2013. Photocatalytic degradation of methyl tert-butyl ether (MTBE) by Fe-TiO<sub>2</sub> nanoparticles. *Journal of Industrial and Engineering Chemistry*, 19, 1697-1702.
- [30] Sawidis, T., Breuste, J., Mitrovic, M., Pavlovic, P. & Tsigaridas, K. 2011. Trees as bioindicator of heavy metal pollution in three European cities. *Environmental Pollution*, 159, 3560-3570.
- [31] Sayyar, Z., Akbar Babaluo, A. & Shahrouzi, J. R. 2015. Kinetic study of formic acid degradation by Fe<sup>3+</sup> doped TiO<sub>2</sub> self-cleaning nanostructure surfaces prepared by cold spray. *Applied Surface Science*, 335, 1-10.
- [32] Serpone, N., Lawless, D., Disdier, J. & Herrmann, J.-M. 1994. Spectroscopic, photoconductivity, and photocatalytic studies of TiO<sub>2</sub> colloids: naked and with the lattice doped with Cr<sup>3+</sup>, Fe<sup>3+</sup>, and V<sup>5+</sup> cations. *Langmuir*, 10, 643-652.
- [33] Sin, J.-C., Lam, S.-M., Mohamed, A. R. & LEE, K.-T. 2011. Degrading Endocrine Disrupting Chemicals from Wastewater by TiO<sub>2</sub> Photocatalysis: A Review. *International Journal of Photoenergy*, 2012.
- [34] SU, Y., Xiao, Y., LI, Y., DU, Y. & Zhang, Y. 2011. Preparation, photocatalytic performance and electronic structures of visible-light-driven Fe-N-codoped TiO<sub>2</sub> nanoparticles. *Materials Chemistry and Physics*, 126, 761-768.
- [35] Sun, S., Ding, J., Bao, J., Gao, C., QI, Z., Yang, X., HE, B. & LI, C. 2012. Photocatalytic degradation of gaseous toluene on Fe-TiO<sub>2</sub> under visible light irradiation: a study on the structure, activity and deactivation mechanism. *Applied Surface Science*, 258, 5031-5037.
- [36] YU, J., Xiang, Q. & Zhou, M. 2009. Preparation, characterization and visible-light-driven photocatalytic activity of Fe-doped titania nanorods and first-principles study for electronic structures. *Applied Catalysis B: Environmental*, 90, 595-602.
- [37] Zhai, J., Wang, D., Peng, L., Lin, Y., LI, X. & Xie, T. 2010. Visible-light-induced photoelectric gas sensing to formaldehyde based on CdS nanoparticles/ZnO heterostructures. *Sensors and Actuators B: Chemical*, 147, 234-240.